NJC

Accepted Manuscript

ROYAL SOCIETY OF CHEMISTRY

rsc.li/njc

View Article Online
DOI: 10.1039/C6NJ02753A

Enhanced cytotoxicity by benzothiazole-containing cisplatin derivative in breast cancer cells

Chaoqun You [a], Jia Yu [a], Yu Sun [a], Yanghui Luo [a], Xiangyang Zhang [b], Jin Zhu [c], Baiwang Sun [a,*]

[a] School of Chemistry and Chemical Engineering, Southeast University, Nanjing 210089, PR China. Fax: +86 25 52090614, Tel: +86 25 52090614, E-mail address: chmsunbw@seu.edu.cn

[b] Laboratory of Organic Chemistry, ETH Zurich, 8093 Zurich, Switzerland

[c] Key Laboratory of Antibody Technique of Ministry of Health, School of Pathology, Nanjing Medical University, Nanjing 210093, PR China

Abstract

In recent years, nanoparticle as an intelligent drug carrier has caused great attention. In this paper, formulation of liposome delivery system loaded with a novel benzothiazole-containing cisplatin derivative (CJM-Pt) was carried out. The particle size distributions were determined by dynamic light scattering and the prepared liposomes showed a suitable size of around 98 nm. Stability study showed the CJM-Pt loaded liposomes were stable at 4℃ for more than four weeks. The investigation of triggered release indicated that the release performance of prepared liposomes were controllable and the releasing effect remarkable under low pH (< pH 6.8) and high temperature (> 42℃). To test suitability of chosen formulation, CJM-Pt loaded liposomes were investigated against several tumor cell lines: MGC-803, SGC-7901, MCF-7 and MDA-MB-231. Furthermore, the cell cycle arrest was examined. The

View Article Online
DOI: 10.1039/C6NJ02753A

CJM-Pt loaded liposomes have the potential to be applied in the drug delivery system (DDS) for breast cancer therapy.

KEYWORDS: cisplatin, benzothiazole, liposomes, drug delivery, synergic action, drug release

1. Introduction

The widely used of cisplatin, carboplatin and oxaliplatin in clinical for cancer therapy has caused great attention to search for more effective cisplatin derivatives, and as a consequence hetaplatin and miriplatin have been successively developed and applied in clinic [1,2]. In particular, cisplatin has played a crucial role for tumor chemotherapy among all the platinum-based drugs, and has reached medicinal chemistry classic around the world [3]. However, the water insoluble and severe side effects of platinum drugs have limited their more extensive application to a great extent. In order to overcome these drawbacks, a series of drug-design strategies have been developed in the past decades [4-11]. Combine platinum derivatives with some other active pharmacophore as one of the most important approaches has been put forward, and a synergic action can be achieved when against the tumor cells [12-15].

The synthesized molecule would break down into two original drug molecules as delivery to the targeted position [16-17]. Samuel G, et al [18] have conjugated D(+)-Tryptophan to Pt(IV) for combined immunomodulation and DNA cross-link-triggered apoptosis for cancer "immune-chemotherapy". Huang Rong, et al [19] has described a novel conjugate comprising of Herceptin (an anti-HER2 antibody) and platinum drug via a cathepsin B cleavable dipetide for enhancing drug

View Article Online
DOI: 10.1039/C6NJ02753A

accumulation and HER2-positive cancer cell specific delivery.

To overcome the water insoluble and severe side effects which limit the efficacy of platinum drugs by countering biological compensation, synergistic combination of platinum-based derivatives with some other active pharmacophore is a promising strategy, which allowing reduced dosage of each agent or accessing context-specific multiple targets [20-23].

Benzothiazole as an active pharmacophore belong to the family of bicyclic heterocyclic compounds having benzene nucleus fused with five-membered ring comprising nitrogen and sulfur atoms. Benzothiazole is an important backstop with a wide range of interesting biological activities and therapeutic functions including resisted some common serious diseases [24-27], remitted inflammation caused by bacteria [28-30], anticonvulsant and analgesic [31-33], anthelmintic [34], and antitumor activities [35]. In particular, a large number of benzothiazole derivatives have shown potent anticancer activity [36]. Some of the recent literature reports are summarized in previous literatures.

A new series of 2-(4-aminophenyl)benzothiazoles has been synthesized by simple, high-yielding routes through substituted in the phenyl ring has been reported [37]. The present molecule CJM126 shows potent inhibitory activity in vitro in the micromole range against a series of human breast cancer cell lines [38], moreover, it has been even used in clinical for tumor therapy in some case [39-40].

Over the past few decades, there has been an increasing interest in the potential use of nanocarriers as delivery supporter for chemotherapeutic drugs and the researches have

View Article Online
DOI: 10.1039/C6NJ02753A

indicated that these nanocarriers can significantly enhance the anti-tumor efficiency for delivery drugs to targeted tissues [41]. Recently, multifunctional delivery systems have been developed for delivery of various guests, including liposomes [42], micelles [43-44], and inorganic nanoparticles [45].

Liposomes can release drugs in an efficacious and controllable way attributed to the good biocompatibility and simple surface functionalization [46-47]. Ashley, et al [48] has reported a nanocarrier by depositing a dioleoyl phosphatidylethanolamine (DOPE) based liposome on mesoporous nanoparticles and observed its pH-dependent release characteristics. Since both the pH value and temperature at the tumor sites are different from those in normal tissues, designing a dual-stimuli-responsive drug carrier achieved the potential for clinical applications [49-58].

In this paper, we have synthesized a novel cytotoxicity molecule by combine two drug molecules though chemical coupling for the first time and using liposome as a carrier for drug delivery. We look forward to the prepared drug loaded liposomes exhibit good cytotoxicity against tumor cells owing to the antitumor property of CJM126 and its possible synergic action with cisplatin. The prepared CJM-Pt loaded liposomes have the potential to be applied in the drug delivery system (DDS) for breast cancer therapy.

2. Materials and methods

2.1 Materials. 2-Benzothiazolamine was purchased from Meryer (Shanghai) Chemical Technology Co., Ltd. Soybean phospholipids (SP), the diblock copolymer of poly (ethylene glycol) with poly (ε-caprolactone)(PEG_{5k}-PCL_{10k}) were purchased from

View Article Online
DOI: 10.1039/C6NJ02753A

Polymtek Biomaterial Co., Ltd (Shenzhen, China). Cisplatin was purchased from Shandong Boyuan Pharmaceutical Co., Ltd (Jinan, Shandong, China). FITC, Hoechst33342 were purchased from Beyotime Biotechnology (Haimen, Jiangsu, China). All other chemical reagents were obtained from Sinopharm Chemical Reagent Co., Ltd.

2.2 Synthesis of benzothiazole containing cisplatin derivative (CJM-Pt) molecules. CJM-Pt molecule was obtained via conjugate CJM126 to cisplatin in aqueous solution under room temperature with three steps [59-60].

2.3 Preparation of CJM-Pt loaded liposomes (Lipo-CJM-Pt). Liposomes encapsulating CJM-Pt were formulated by the film hydration method as reported by literature with slight modifications [61]. Briefly, SP (45mg), PEG-PCL (2mg), CJM-Pt (15mg) was dissolved in acetonitrile (40ml), and a thin film was formed by solvent evaporation under reduced pressure. The acetonitrile was removed completely by placing the flask overnight in a vacuum desiccator. Then deionized water (40ml) was added to the copolymer film and ultrasonic vibration for 5 min. Suspension was shaken for 30 min at 30℃ to ensure well dispersed. Formulation was then centrifuged at 3000 RCF for 15 min and filtered using a 0.22μm filter (Millipore) and lyophilized.

2.4 Liposome Characterization.

Particle size analysis. Particle size distribution was estimated by dynamic light scattering (DLS) and the sample of the stepwise extrusion through 0.22μm membranes after ultrasonic vibration for 5 min. Each sample was diluted 2-fold with ultrapure water before measurement and analyzed in triplicate at 25℃. The particle

View Article Online
DOI: 10.1039/C6NJ02753A

size distribution data were generated using the DTS nano software (version 5.2). The liposome size polydispersity was expressed by the polydispersity index, PDI.

Zeta potential. The ζ potential was determined using a Malvern Zetasizer Nanoseries (Malvern Instruments Zen 3600, Malvern, U.K.) and measurements were performed at least three times after dilution in water. The ζ potential was calculated by the electrophoretic mobility applying the Helmholtz-Smoluchowski equation.

Transmission Electrom Microscopy (TEM). Particle morphology was detected by a JEM-100CXII transmission electron microscopy (TEM).

2.5 The entrapment efficiency and drug loading capacity in Lipo-CJM-Pt. The Lipo-CJM-Pt was prepared under specific conditions as the literature described thin-film hydration method [62]. The purified drug-loaded liposomes were freeze-dried. The CJM-Pt mass loaded in liposomes was calculated by a High Performance Liquid Chromatograph at 293 nm (comparing with CJM-Pt calibration curve) after extracting CJM-Pt from the dried drug-loaded liposomes with methanol. The entrapment efficiency and drug loading capacity were calculated according the following equations:

$$\text{EE (\%, CJM-Pt)} = \frac{\text{weight of CJM-Pt in liposomes}}{\text{initial weight of CJM-Pt}} \times 100\%$$

$$\text{DLC (\%, CJM-Pt)} = \frac{\text{weight of CJM-Pt in methanol}}{\text{weight of drug loaded liposomes}} \times 100\%$$

2.6 The stability of liposomes [63]. The prepared liposomes were stored at 4℃ for up to 4 weeks. The stability of prepared liposomes was evaluated on Days 0, 7, 14, 21and 28. At each time point, the liposomal samples were centrifuged at 1200 RCF for 15 min to ensure that the leaked CJM-Pt content was sedimented. Then 5mL aliquot was

View Article Online
DOI: 10.1039/C6NJ02753A

taken separately from each supernate, microfuged and mixed with 10mL methanol, and then centrifuged at 1500 RCF for 15min, precipitation dissolved in methanol 10ml and the CJM-Pt content was quantified for each time point (in triplicates) by HPLC.

2.7 In vitro multiple triggered release of liposomes. CJM-Pt released from Lipo-CJM-Pt was performed by detecting the platinum content as released from the liposomes [64]. We tested pH (7.4, 6.8, 6.2, 5.5, 5.0) and temperature (32, 35, 37, 39, 42, 45℃) triggered release of liposomes. An amount of 2 mL of Lipo-CJM-Pt solution was achieved from the flask at given condition. The solution was centrifuged at 1200 RCF for 15 min to ensure that the leaked CJM-Pt content was sedimented. Then the supernate was collected. After filtered using a 0.22μm filter for 2 times in the dark, the CJM-Pt mass loaded in liposomes was calculated by a High Performance Liquid Chromatograph at 293 nm.

To investigate the pH-dependent releasing efficiency, three aliquots of the CJM-Pt loaded nanoparticles with equal amount were immersed in 3 mL of buffer solution at 25℃ with pH = 7.4, pH = 6.8, pH = 6.2, pH = 5.7 and pH = 5.0, respectively. The mixture was shaken at certain time intervals. The supernatant was taken out by centrifugation to measure the absorption, and an equal volume of fresh medium was added instead. By comparing the absorption curve of pure CJM-Pt in different pH solutions, the amount of released CJM-Pt can be calculated.

To investigate the thermal stimuli release efficiency of the prepared carrier, three aliquots of Lipo-CJM-Pt with equal amount were immersed in 3 mL of PBS buffer

View Article Online
DOI: 10.1039/C6NJ02753A

(pH = 7.4) at T = 25℃, T = 37℃, T = 42℃, and T = 45℃. The procedure of absorption measurement was the same as that of a pH-dependent release investigation.

2.8 Cell cultures. MGC-803 and SGC-7901 human gastric carcinoma cells were cultured in RPMI 1640 medium, MCF-7 and MDA-MB-231 human breast cancer cells were cultured in Dulbecco's Modified Eagle medium (DMEM). Both media were supplemented with 10% heat-inactivated fetal bovine serum (FBS), and 1% Antibiotic/Antimycotic solution. All cell lines were incubated at 37℃ in a humidified incubator in a 5% carbon dioxide atmosphere.

2.9 In vitro cytotoxicity. Cytotoxicity of prepared liposomes was evaluated by MTT assay with MGC-803, SGC-7901, MCF-7 and MDA-MB-231 cells. The cells were seeded into a 96-well plate for 24 h (5×10^3 cells/well) and incubated at 37℃ with 5% CO_2. The supernatants were discarded, and the cells were washed twice with PBS (pH=7.4). Free CJM-Pt and CJM-Pt loaded liposomes (Lipo-CJM-Pt) were equivalently put into the culture medium for 24 h at a certain concentration of 3, 6, 12, 24, or 48μg/mL, respectively. The complete medium without cells was put in the wells for blank groups and the culture medium without CJM-Pt (PBS) but contain 5% DMSO was put in the wells for control groups. Then 20μL of MTT solution (5.0 mg/mL) was added to each well, and the cells were further incubated for 4h at 37 °C. Next, the medium was removed, and then 150μL of dimethyl sulfoxide (DMSO) was put in the well to dissolve the formazan crystals formed by the living cells. The absorption was recorded at 490 nm using a microplate reader (Thermo Scientific Varioskan Flash, Waltham, MA, USA). The in vitro toxicity of free CJM-Pt,

View Article Online
DOI: 10.1039/C6NJ02753A

CJM-Pt-loaded and blank liposomes were expressed as cell viability, defined by the following equation：

$$\text{Cell viability} = \frac{A1-A0}{A2-A0} \times 100\%$$

Where A0 was the absorbance of the complete medium without cells, A1 was the absorbance of the cells incubated with different formulations (the presence of CJM-Pt concentration of 3, 6, 12, 24, or 48μg/mL for 24h) and A2 was the absorbance of the control groups.

2.10 Cellular uptake study. Intracellular delivery of Lipo-CJM-Pt and co-localization of CJM-Pt and the nucleus were observed by laser confocal microscope. MGC-803, SGC-7901, MCF-7 and MDA-MB-231 cells were cultured until 70~80% confluency and then trypsinized, seeded onto confocal petri dish (BD Falcon, USA) at a density of 1.0×10^5 cells/well. After the cells were incubated for 24h at 37℃, Lipo-CJM-Pt with equivalent concentration of FITC at 1.0 mg/mL dissolved in 1640 or DMEM were added and incubated for further 24h at 37℃ along with complete medium as negative control. Hoechst 33342 in 1640 or DMEM were added to stain nuclei and cells were incubated for 12h, respectively. All reagents were removed after incubation and cells were washed with PBS (pH=7.4) three times. Mounting medium was added to prevent quenched and fixed the cells. Cells were observed by laser confocal microscope (Zeiss, Germany)

2.11 Cell apoptosis and cycle arrest.

Cell apoptosis. Annexin staining for measurement of apoptosis was performed using the APC/7-AAD Apoptosis Detection Kit II (BD Pharmingen, San Jose, USA). Briefly,

View Article Online
DOI: 10.1039/C6NJ02753A

MGC-803, SGC-7901, MCF-7, MDA-MB-231 cells were seeded at 1×10^5 cells/dish and incubated for 24h. The cells were then treated with 50μM CJM-Pt as CJM-Pt loaded liposomes. Blank-liposomes served as blank. After 24h of treatment, cells were washed with cold PBS and resuspended in 200μL binding buffer. Cells were stained with 10μL of APC and 5μL of 7-AAD for 15 min in the dark before diluting with an additional 300 ml binding buffer. Samples were analyzed by flow cytometry on a FACS Calibur (BD Biosciences, USA).

Cell cycle arrest. 1×10^6 MDA-MB-231 cells were treated with CJM126, CJM-Pt and cisplatin for 48h with complete medium free from drugs as negative control. Then cells were collected and washed with PBS. After centrifugation, the cell suspensions were fixed by addition of 70% ethanol overnight at 4℃. For staining, cells were centrifuged, resuspended in PBS, treated with DNA staining for 30 min in the dark. The cells were analyzed with a FACS Calibur (BD Biosciences, USA)

3. Results and discussion

3.1 Synthesis of CJM-Pt molecules. We designed and synthesized the hybrid compounds by combine CJM126 molecule with cisplatin via a malonyl dichloride linker, the scheme of reaction route was show in Fig. 1. The yellowish green product was subsequently purified from methanol, and dried in vacuo with a yield of 22%.

^{1}HNMR displayed clearly peaks characteristic of CJM126, CJM-COOH and CJM-Pt (Fig. S1). The data indicated that integral ratio between resonances at s 10.061 (carboxyl protons in the head of CJM-COOH) and d 3.686 (methylene protons of malonyl dichloride skeleton) was nearly to the theoretical value of 1:2(Fig. S1a, 1b),

View Article Online
DOI: 10.1039/C6NJ02753A

which confirming successful synthesis of CJM-COOH. The ^{1}HNMR data also shows complete disappearance of signal at d 10.061 due to carboxyl protons reacted with the equimolar barium salt, and no new set of signals come out assignable to the formatiom of CJM-Pt (Fig. S1c). The Mn values of CJM-Pt could be estimated by comparing the intensities of signals at d 10.601 and 3.965 which were attributable to the carboxyl protons belong to the ester bonds of CJM-COOH and the thiazole ring protons next to the ester bonds of CJM-Pt, respectively.

3.2 Preparation and characterization of liposomes. Liposomes were prepared under sterile conditions as the literature described thin-film hydration method. The schematic diagram of prepared Lipo-CJM-Pt was shown in Fig. 2. To prepare the liposomes with a suitable size and perfect morphology, we carried out a series of experiments with different supply proportion. Through change the supply proportion and the reaction time of dissolution-emulsification self-assembled, we achieved liposomes with relative excellent sizes suitable for in vivo transportation. The prepared liposomes have a uniform spherical shape with a mean size of about 98nm as shown in Fig. 3A, this result attributed to the addition of phospholipids by enhance the stability of prepared liposomes. The TEM study indicated that the prepared liposomes show an excellent size and a uniform spherical shape as shown in Fig. 3C. The results also show that the average diameters of CJM-Pt loaded liposomes were about 98 nm and which emphasize the well dispersed state of the liposomes by representative particle size and homogeneity morphology. The results also suggested the surface of prepared liposomes (Lipo-CJM-Pt) was relatively smooth. The tested

View Article Online
DOI: 10.1039/C6NJ02753A

results of the ζ potential was suggested that the zeta potential on the surface of Lipo-CJM-Pt tended to be neutral may due to not conjugated liposomes with any ligands, such as polymer chain , micro molecule polypeptide or the antibody (Fig. 3B). Fig. 3D shows the morphological changes of a liposomes solution of different concentrations, liposomes solution overall brown and gray, furthermore the solution color and the concentration were correlated positively.

The typical recipes and tested results were listed in Table S1. Table S1 demonstrated the important characteristics of the liposomes, including mean diameter, encapsulation efficiency (EE), drug loading capacity (DLC) and polydispersity index (PDI) value. All of the liposomes showed good homogeneity, with PDIs below 0.30 and mean particle sizes between 73.39 and 117.30 nm. From Table S1, we found that the particle sizes of liposomes increased from 73.39 to 117.30 nm on DLS as increase the ratio of phospholipids, the polydispersity index (PDI) of DLS was keep blow 0.3, which meant that the liposomes show homogeneity morphology.

To investigate the entrapment efficiency and drug loading capacity in Lipo-CJM-Pt, liposomes were prepared as reported previously [65-68]. Then the entrapment efficiency and drug loading capacity in Lipo-CJM-Pt were calculated by detected the CJM-Pt mass in liposomes with a High Performance Liquid Chromatograph at 293 nm (comparing with CJM-Pt calibration curve) after extracting CJM-Pt from the dried drug-loaded liposomes with methanol as well.

3.3 The stability of liposomes. The liposomal preparations were stored at 4℃ for up to 4 weeks. The stability of liposomal preparations was evaluated on Days 0, 7, 14,

View Article Online
DOI: 10.1039/C6NJ02753A

and 21. At each time point, the liposome samples were centrifuged at 1200 RCF for 15 min to ensure that the leaked CJM-Pt content was sedimented. Then 25mL supernatant was taken out and mixed with 50mL methanol separately, centrifuged and the CJM-Pt content was calculated on each time point (in triplicates) by HPLC at 293nm (comparing with CJM-Pt calibration curve), as the result show in Fig. 4.

The stability of CJM-Pt loaded liposome formulation was monitored during storage for four weeks at 4℃. The results demonstrated that a large portion of liposomes retained CJM-Pt without significant leakage and the prepared liposomes show excellent stability as show in Fig. 4A. Generally, as for storage at 4℃，the retention of CJM-Pt in the liposomes was reduced to 11.29%，11.24%，11.19%，11.07% by the 1st, 2nd, 3rd and 4ur week, respectively. At the same time the particle size and the encapsulation efficiency showed little change, the PDI parameters remain in a good level. This result shows that the prepared liposomal formulation can be stored for a certain period with an excellent stability.

3.4 In vitro pH triggered release of liposomes. A CJM-Pt loaded liposomes solution was divided into five aliquots and the pH of each aliquot was adjusted to 5.0, 5.7, 6.2, 6.8 and 7.4. To investigate the pH-dependent releasing efficiency, five aliquots of CJM-Pt loaded liposomes with equal amount were immersed in 3mL of buffer solution at 25℃ with pH = 7.4, pH = 6.8, pH = 6.2, pH = 5.7 and pH = 5.0, respectively. The mixture was shaken at certain time intervals. The supernatant was taken out to measure the CJM-Pt content after centrifugation, and an equal volume of fresh medium was added instead. By comparing the absorption value of the CJM-Pt

View Article Online
DOI: 10.1039/C6NJ02753A

calibration curve, the amount of released CJM-Pt can be calculated.

The results showed the liposomes express sensitively pH trigged release as demonstrated in Fig. 4B. The release process of the Lipo-CJM-Pt was monitored at certain time intervals within 24h at 25℃. As show in Fig. 4B, the amounts of released CJM-Pt increased along with reduced the pH value. Specifically, about 41.27% of CJM-Pt was released at pH = 7.4 when about 83.00% of CJM-Pt was released at pH = 6.8 in 24h. Furthermore, the released amount of CJM-Pt significantly increased to about 97.65% at pH = 5.0, which more than 2-fold as compared with it at pH = 7.4. This is because lipid bilayer of the phospholipids added little PEG-PCL structure exhibits a compact arrange state at some degree under neutral pH conditions, which transforms to a hydrophilic chain structure while reduced the pH value. Such a change of morphological structure on the phospholipid bilayer impacts the barrier property of liposomes. The release efficiency in 24h was 41.27%, 83.00%, 88.50%, 94.72% and 97.65% corresponding to pH 7.4, pH 6.8, pH 6.2, pH 5.5 and pH 5.0, respectively.

Thus, the different pH value demonstrated obviously effect on the releasing of Lipo-CJM-Pt. As a consequent, the prepared CJM-Pt loaded liposomes exhibited a quite remarkable pH-controllable property with the PEG-PCL mediated lipid bilayer. This is of great valuable in vivo applications of pH-responsive nanocarriers because of the low pH environment of cancer cells than that of the normal ones.

3.5 In vitro temperature triggered release of liposomes. The investigated of temperature triggered release of liposomes was the same procedure as that of the pH triggered. Investigated with different temperature degree by 25℃, 30℃, 37℃, 42℃,

View Article Online
DOI: 10.1039/C6NJ02753A

45℃of buffer solution at pH = 7.4.

As the pH-controllable release performance was achieved previously, the thermo-controllable release characteristic was studied. As shown in Fig. 4C, the phase transition temperature (Tm) of the prepared liposome is around 42℃ at pH 7.4. Therefore, the release curves at four different temperatures (25℃, 37℃ (T < Tm), 42℃ (T = Tm), and 45℃ (T > Tm)) were obtained with certain pH value at 7.4 in our study. The achieved results are show in Fig. 4C. The releasing efficiency of CJM-Pt at 42℃ (Tm) reached 85.90% after 24 h, which is remarkable higher than those at the lower temperatures (57.52% at 25℃ and 81.28% at 37℃). Moreover the releasing efficiency of CJM-Pt at 45℃ reached 92.59% after the same time. The results consistent with the property of the liposomes as described by the previously literatures. The possible explanation may as follows. Briefly, as the temperature is below Tm, the contained CJM-Pt was leaked from the gap of the composite bilayer. However, when the temperature reaches the Tm value of the composite bilayer, the PEG-PCL mediated phospholipids structure could be depolymerized and fall to pieces under high temperature. When the temperature increased to be higher than Tm, the hydrophobic structure of liposomes become more depolymerized and even to the surface, which accelerated the release of CJM-Pt from the liposomes core. The achieved results indicated that the prepared liposomes show a thermo-responsive releasing ability.

3.6 In vitro cytotoxicity. A remarkable attention to nanomaterials for bio-application is their toxicity, therefore, the cytotoxicity of CJM126 and CJM-Pt toward tumor cells

View Article Online
DOI: 10.1039/C6NJ02753A

were investigated with the standard MTT assays, and then the IC_{50} (μg/mL) for each cell culture were calculated as show in Table S2. Each sample was diluted 2-fold with ultrapure water before measurement and analyzed in triplicate at 25℃.

The IC_{50} (μg/mL) for MGC-803, SGC-7901, MCF-7 and MDA-MB-231 cell lines were investigated and the results were shown in Table S2. Among these cell lines, CJM126 was more toxicity to MDA-MB-231 particularly. The IC_{50} of CJM-Pt was 38.36% less than cisplatin while the IC_{50} of CJM126 was nearly double of cisplatin, which indicated that CJM126 and cisplatin enhance synergistically in cytotoxicity against MDA-MB-231 through the combination.

Furthermore, to investigate whether the cancer cells can be efficiently inhibited by Lipo-CJM-Pt, we incubated the CJM-Pt loaded liposomes with MGC-803, SGC-7901, MCF-7, MDA-MB-231 cells for 24h at 37℃, and then the cytotoxicity of Lipo-CJM-Pt towards tumor cells was investigated with the standard MTT assays (Fig. 5). The liposomes were diluted with 1640 or Dulbecco's Modified Eagle's medium (DMEM) and incubated with MGC-803, SGC-7901, MCF-7 and MDA-MB-231 cells in 5% CO_2 at 37℃ for 24h. According to all the Blank-liposomes, the cytotoxicity slightly increases with increasing liposomes concentration. As for human gastric cancer cells, no significant cytotoxicity was observed in cells when the concentration of Blank-liposomes was less than 48μg/mL, and the cell viability remained above 80% except 70.82% of MGC-803 at 48μg/mL. The results indicate that the prepared liposomes have low cytotoxicity for gastric cancer cells under the current drug concentration.

View Article Online
DOI: 10.1039/C6NJ02753A

Next, we further investigated the cytotoxicity of Lipo-CJM-Pt against human breast cancer cells with the MCF-7 and MDA-MB-231cells. The cytotoxicity of free cisplatin, Blank-liposomes and Lipo-CJM-Pt was investigated in MCF-7 and MDA-MB-231 cell lines, and the anticancer effect was studied by MTT assay as well. CJM-Pt shows concentration of positive correlations on the cell viability of both MCF-7 and MDA-MB-231 cells lines after dose for 24h as show in Figs. 5C and 5D.

However, the liposomes shell structure reduced the cytotoxicity of CJM-Pt against MGC-803 cells and maintained the cell viability to over 45% even increasing the equivalent concentration of Lipo-CJM-Pt (Fig. 5A). Furthermore, the inhibitory effect on the cell viability of SGC-7901 cells was time-dependent. There was no remarkable viability change in SGC-7901 cells when treated with Blank-liposomes (Fig. 5B). Although the cytotoxicity was diminished using CJM-Pt loaded liposomes against SGC-7901 cells, Lipo-CJM-Pt showed dose-dependent inhibitory effect and inhibited the proliferation of MCF-7 cells to less than 57% after treatment for 24h in 48mg/mL of equivalent concentration of Lipo-CJM-Pt (Fig. 5C). The inhibitory effect on the proliferation of MDA-MB-231 maintained at 74% for 24h (Fig. 5D). The results indicated that when Lipo-CJM-Pt came into contact with the MDA-MB-231, more quantity were absorbed by cells and demonstrated higher cell inhibition. However the inhibitory effect of Lipo-CJM-Pt was obviously cannot be comparable to free CJM-Pt in 24h.

3.7 In vitro cellular uptake assay. In this study, the cellular uptake efficiency of Lipo-CJM-Pt was evaluated by confocal laser scanning microscopy (CLSM). As show

View Article Online
DOI: 10.1039/C6NJ02753A

in Fig. 6, only a few of Lipo-CJM-Pt (green fluorescence signed) was focused on the nucleus in MGC-803 cells and SGC-7901 cells after incubated for 12h, which was consistent with the cytotoxicity results. The remarkable strong green fluorescence in the nucleus of MCF-7 cells with Lipo-CJM-Pt treated (compared to the human gastric cancer cells) indicated the intracellular uptake was enhanced by Lipo-CJM-Pt. In particular, Lipo-CJM-Pt showed the highest intracellular uptake in MDA-MB-231 cells (with strongest green fluorescence intensity), which was almost cover the whole field of view. However, the fluorescence intensity indicated no remarkable difference between MCF-7 and MDA-MB-231 for human breast cancer cells. These results indicated that human breast cancer cells effectively internalized the CJM-Pt loaded liposomes by the cell endocytosis.

Based on the previous cellular uptake experiments, the possible mechanism of cellular uptake enhancement for the CJM-Pt loaded liposomes was as follows: Due to the good biocompatibility of composite material liposomes, it can release drugs in an efficient way. The excellent biocompatibility of the CJM-Pt loaded liposomes was delivery to the tumor cells; the drug in liposomes rapidly released when subjected to low pH or hyperpyrexia and then spread into the tumor along the drug concentration gradient.

3.8 Cell apoptosis and cycle arrest. To further evaluate the induced apoptosis effect of the Lipo-CJM-Pt on tumor cells, the annexin staining for measurement of apoptosis was performed with the APC/7-AAD Apoptosis Detection Kit, the prepared cells were sorted by flow cytometry. To compare the apoptosis rate between human gastric

View Article Online
DOI: 10.1039/C6NJ02753A

cancer cells and breast cancer cells, MGC-803, SGC-7901, MCF-7 and MDA-MB-231 cells were cultivated. After the cell cultures were treated with Lipo-CJM-Pt for 24 h, the apoptotic cells were detected by flow cytometry as shown in Fig. 7, Blank-liposomes did not induce obvious apoptosis for all and only induced less than 10% apoptosis especially in MCF-7 cells the data only 6.0%. Meanwhile, the blank liposomes treatment to MGC-803 induced alone only around 10.6%.

The Lipo-CJM-Pt mediated apoptosis, which was remarkable higher than treatment with blank liposomes alone. All the induced apoptosis occurred at the early apoptosis, related to the inductive effect on the apoptosis of cancer cells was time-dependent. The apoptosis rate of MDA-MB-231 reached 60.2% as higher than MCF-7 (47.8%) and MGC-803 (46.6%). In particular, this obtained results demonstrated that the Lipo-CJM-Pt show the minimal impact to SGC-7901 with only 40.8% degree. These results suggest that treatment with CJM-Pt loaded liposomes can overcome resistance of breast cancer cells. However, the Lipo-CJM-Pt treatment induced more than 1.2-fold increase in apoptosis for breast cancer cells when compared with Lipo-CJM-Pt treatment of gastric cancer cells on the whole. This suggested that the prepared liposomes more suitable for resistance of human breast cancer cells.

To further investigate the cell cycle arrest induced by CJM126 and CJM-Pt, the cell cycle distribution of MDA-MB-231 cells treated with CJM126 and CJM-Pt were detected by flow cytometry under the PI staining with cisplatin for comparison. As shown in Fig. 8, cisplatin strongly interfere with the cell cycle in S phase. The cell percentage at S phase obviously increases from 19.01% to 23.10%, with a decrease of

View Article Online
DOI: 10.1039/C6NJ02753A

cell percentage at G0/G1 phase from 75.83% to 74.81% which highly consistent with the general consensus that cisplatin acts as a DNA binding agent to prevent DNA replication [69]. CJM-Pt also induces the cell cycle remarkably as compared with control group. In particularly, the cell percentage at G0/G1 phase decreased and those at G2/M phase decrease from 5.16% to 1.83% as well. As for CJM126, the cell percentage at G0/G1 phase decrease, while those at G2/M phase increase from 5.16% to 6.63%. It indicates that CJM126 remarkable induces cell cycle arrest mainly at G2/M phase. Based on the previous cell cycle experiments, the proposed mechanism of effect on cell cycle for the CJM-Pt molecule was as follows: As the CJM-Pt released from Lipo-CJM-Pt in the cancer cells, the CJM-Pt molecule break down into CJM126 and cisplatin with the cleavage of chemical bonds. So it suggested that CJM-Pt acted as a derivative from cisplatin may have changed its DNA binding mode and result in a different cell cycle arrest from cisplatin. It also indicated that it achieved the synergistic effect from the CJM-Pt molecule.

4. Conclusions

A synergic actional cisplatin derivative via conjugated CJM126 with cisplatin was successfully synthesized and delivery by liposomes for cancer treatment in this study. The prepared drug loaded liposomes show suitable size around 98nm and a spherical morphology. The entrapment efficiency and drug loading capacity in prepared liposomes reached 75% and 31%, respectively. And the present liposomes also demonstrated an excellent stability by retained cisplatin derivative without significant leakage for four weeks.

View Article Online
DOI: 10.1039/C6NJ02753A

The investigated of pH and temperature triggered release of liposomes indicated that the release of prepared liposomes was controllable and the releasing effect remarkable under low pH (< pH 6.8) and high temperature (> 42℃). The cisplatin derivative molecule demonstrated good cytotoxicity as compared with cisplatin, especially the IC_{50} (μg/mL) less than 17.47 (the IC_{50} of cisplatin) for MDA-MB-231. As compared with human gastric cancer cells, the prepared drug loaded liposomes showed more cytotoxicity to human breast cancer cells. The cellular uptake in vitro result showed that the prepared nanocarriers were internalized by tumor cells obviously owing to the good biocompatibility of liposomes. The cisplatin derivative molecule induced more than 1.2-fold increase in apoptosis for breast cancer cells when compared with the treatment of gastric cancer cells on the whole. This suggests that the prepared cisplatin derivative loaded liposomes could achieve better chemotherapy efficiency on human breast cancer cells. The cell cycle study indicates that CJM126 obviously induces cell cycle arrest mainly at G2/M phase. To sum up, the current studies indicate that the cisplatin derivative loaded liposomes have the potential to be applied in the drug delivery system (DDS) for human breast cancer therapy.

Acknowledgments

We are highly grateful to the financial support from the National Natural Science Foundation of China (Nos. 21628101 and 21371031), the International S&T Cooperation Program of China (No. 2015DFG42240) and the Priority Academic Program Development （PAPD）of Jiangsu Higher Education Institutions.

View Article Online
DOI: 10.1039/C6NJ02753A

Supporting Information

Synthesis, characterization, IC_{50} values and relevant testing curve.

References

1. B. Rosenberg, L. Van Camp and T. K. Rigas, *Nature.* 1965, **205**, 698-699.
2. P. Marques-Gallego, H. Dulk, J. Brouwe, H. Kooijman, A. L. Spek, O. Roubean, S. J. Teat and J. Reedijk, *Inorg. Chem.*2008*,* **47**, 11171-11179.
3. J. Reedijk, *Eur. J. Inorg. Chem.* 2009, **10**, 1303-1312.
4. G. Alves, L. Morel, M. E. Ghozzi, D. Avignant, B. Legeret, L. Nauton, F. Cisnetti and A. Gautier, *Chem. Commun.* 2011, **47**, 7830-7832.
5. Y. Yu, S. Domianello, A. A. Legin, M. A. Jakupec, V. B. Arion, V . Y. Kukushkin, M. Galanski and B. K. Keppler, *Inorg. Chem.* 2011, **50**, 10673-10681.
6. J. J. Wilson and S. J. Lippard, *Inorg. Chem.* 2011, **50,** 3103-3115.
7. Y. Min, C. Mao, D. Xu, J. Wang and Y. Liu, *Chem. Commun.* 2010, **46,** 8424-8426.
8. N. J. Farrer, J. A. Woods, L. Salassa, Y. Zhao, K. S. Robinson, G. Clarkson, F. S. Mackay and P. J. Sadler, *Angew. Chem., Int. Ed.* 2010, **49,** 8905-8908.
9. N. S. Bryce, J. Z. Zhang, R. M. Wham, N. Yamamoto and T. W. Hambley, *Chem. Commun.* 2009, **19,** 2673-2675.
10. S. Dhar, Z. Liu, J. Thomale, H. Dai and S. J. Lippard, *J. Am. Chem. Soc.* 2008, **130,** 11467-11476.
11. A. Hegmans, S. J. Berners-Price, M. S. Davies, D. S. Thomas, A. S. Humphreys and N. Farrell, *J. Am. Chem. Soc.* 2004, **126,** 2166-2180.

View Article Online
DOI: 10.1039/C6NJ02753A

12. W. H. Ang, I. Khalaila, C. S. Allardyce, L. Juillerat-Jeanneret and P. J. Dyson, *J. Am. Chem. Soc.* 2005, **127,** 1382-1383.

13. J. Ruiz, C. Vicente, C. Deharo and A. Espinosa, *Inorg. Chem.* 2011, **50,** 2151-2158.

14. D. Griffith, M. P. Morgan and C. J. Marmion, *Chem. Commun*. 2009, **44,** 6735-6737.

15. Z. Xue, M. Lin, J. Zhu, J. Zhang, Y. Li and Z. Guo, *Chem. Commun.* 2010, **46,** 1212-1214.

16. H. H. Xiao, R. G. Qi and S. Liu, *Biomaterials.* 2011, **32**, 7732-7739.

17. A. Santosh, M. Chen, H. Jack and L. F. Zhang, *ACS nano.* 2010, **4,** 251-258.

18. G. A. Samuel, Y. R. Zheng and M. B. Peter, *J. Am. Chem. Soc.* 2015, **137,** 14854-14857.

19. R. Huang, Q. C. Wang, X. Y. Zhang, J. Zhu and B. W. Sun, *Biomedicine & Pharmacotherapy.* 2015, **72,** 17-23.

20. J. Lehar, A. S. Krueger, W. Avery, A. M. Heilbut, L. M. Johansen and E. R. Price, *Nat Biotechnol.*2009, **27,** 659-666.

21. J. R. Sharom, D. S. Bellows and M. Tyers, *Curr Opin Chem Biol.* 2004, **8,** 81-90.

22. J. W. G. Kaelin, *Nat Rev Cancer.* 2005, **5,** 689-698.

23. C. T. Keith, A. A. Borisy and B. R. Stockwell, *Nat Rev Drug Discov.* 2005, **4,** 71-78.

24. V. N. Telvekar, V. K. Bairwa, K. Satardekar and A. Bellubi, *Bioorg. Med. Chem. Lett.* 2012, **22,** 649-652.

View Article Online
DOI: 10.1039/C6NJ02753A

25. R. V. Patel, P. K. Patel, P. Kumari, D. P. Rajani and K. H. Chikhalia, *Eur. J. Med. Chem.* 2012, **53,** 209-225.

26. K. N. Venugopala, M. Krishnappa, S. K. Nayak, B. K. Subrahmanya, J. P. Vaderapura, R. K. Chalannavar, R. M. Gleiser and B. Odhav, *Eur. J. Med. Chem.* 2013, **65,** 295-303.

27. G. Mariappan, P. Prabhat, L. Sutharson, J. Banerjee, U. Patangia and S. Nath, *J. Korean Chem. Soc.* 2012, **56,** 251-256.

28. S. Bondock, W. Fadaly and M. A. Metwally, *Eur. J. Med. Chem.* 2010, **45,** 3692-3701.

29. V. S. Padalkar, V. D. Gupta, K. P. Phatangare, V. S. Patil, P. G. Umape, N. Sekar and J. Saudi, *Chem. Soc*. 2011, **4**, 262-268.

30. C. Praveen, A. N. Kumar, P. D. Kumar, D. Muralidharan and P. T. Perumal, *J. Chem. Sci.* 2012, **124,** 609-624.

31. V. G. Ugale, H. M. Patel, S. G. Wadodkar, S. B. Bari, A. A. Shirkhedkar and S. J. Surana, *Eur. J. Med. Chem.* 2012, **53,** 107-113.

32. A. Zablotskaya, I. Segal, A. Geronikaki, T. Eremkina, S. Belyakov, M. Petrova, I. Shestakova, L. Zvejniecea and V. Nikolajeva, *Eur. J. Med. Chem.* 2013, **70,** 846-856.

33. M. A. Azam, L. Dharanya, C. C. Mehta and S. Sachdeva, *Acta Pharm.* 2013, **63,** 19-30.

34. S. Sarkar, J. Dwivedi and R. Chauhan, *J. Pharm. Res.* 2013, **7,** 439-442.

35. J. Cai, M. Sun, X. Wu, J. Chen, P. Wang, X. Zong and M. Ji, *Eur. J. Med. Chem.*

View Article Online
DOI: 10.1039/C6NJ02753A

2013, **63,** 702-712.

36. M. M. Choi, E. A. Kim, H. G. Hahn, K. D. Nam, S. J. Yang, S. Y. Choi, T. U. Kim, S. W. Cho and J. W. Huh, *Toxicology.* 2007, **239,** 156-166.
37. K. G. Rupinder, K. R. Ravindra and B. Jitender, *Arch. Pharm. Chem. Life Sci.* 2015, **348,** 155-178.
38. D. F. Shi, D. B. Tracey, W. Samantha, J. M. Carol, L. Peter, F. Iduna and M. F. G. Stevens, *J. Med. Chem.* 1996, **39,** 3375-3384.
39. C. O. Leong, M. Gaskell, E. A. Martin, R. T. Heydon, P. B. Farmer, M. C. Bibby, P. A. Cooper, J. A. Double, T. D. Bradshaw and M. F. G. Steven, *Br. J. Cancer.* 2003, **88,** 470-477.
40. T. D. Bradshaw, S. Wrigley, D. F. Shi, R. J. Schultz, K. D. Paull and M. F. G. Stevens, *Br. J. Cancer.* 1998, **77**, 745-752.
41. T. M. Sun, Y. S. Zhang, B. Pang, C. H. Dong, M. X. Yang and Y. N. Xia, Angew. Chem., Int. Ed. 2014, **53**, 12320-12364.
42. L. Fan, F. Li, H. Zhang, Y. Wang, C. Cheng and X. Li, *Biomaterials.* 2010, **31,** 5634-5642.
43. A. L. Lee, Y. Wang, H. Y. Cheng, S. Pervaiz and Y. Y. Yang, *Biomaterials.* 2009, **30,** 919-927.
44. H. Wang, P. Zhao, W. Su, S. Wang, Z. Liao and R. Niu, *Biomaterials*. 2010,**31,** 8741-8748.
45. M. Saad, O. B. Garbuzenko and T. Minko, *Nanomedicine.* 2008, **3,** 761-776.
46. A. M. Chen, M. Zhang, D. Wei, D. Stueber and O. Taratula, T. Minko, *Small*.

View Article Online
DOI: 10.1039/C6NJ02753A

2009, **5,** 2673-2677.

47. D. Peer, P. C. Zhu, C. V. Carman, J. Lieberman and M. Shimaoka, *Proc. Natl. Acad. Sci.* 2007, **104,** 4095-4100.

48. M. E. Davis, Z. Chen and D. M. Shin, *Nat. Rev. Drug Discovery.* 2008, **7,** 771-782.

49. C. E. Ashley, E. C. Carnes, G. K. Phillips, D. Padilla, P. N. Durfee, P. A. Brown, T. N. Hanna, J. W. Liu, B. Phillips, M. B. Carter, N. J. Carroll, X. M. Jiang, D. R. Dunphy, C. L. Willman, D. N. Petsev, D. G. Evans, A. N. Parikh, B. Chackerian, W. Wharton, D. S. Peabody and C. Brinker, *J. Nat. Mater.* 2011, **10,** 389-397.

50. Z. M. Xing, C. L. Wang, J. Yan, L. Zhang, L. Li and L. S. Zha, *Soft Matter.* 2011, **7**, 7992-7997.

51. T. Kaiden, E. Yuba, A. Harada, Y. Sakanishi and K. Kono, *Bioconjugate Chem.* 2011, **22,** 1909-1915.

52. J. Zhang, M. Zhang, K. Tang, F. Verpoort and T. Sun, *Small.* 2013, **13**, 1-15.

53. S. Mashaghi, T. Jadidi, G. Koenderink and A. Mashaghi, Int. J. Mol. Sci. 2013, **14**, 4242-4282.

54. X. Zhang, P. Yang, Y. Dai, P. A. Ma, X. Li, Z. Cheng, Z. Hou, X. Kang, C. Li and J. Lin, *Adv. Funct. Mater.* 2013, **23,** 4067-4078.

55. X. Hu, X. Hao, Y. Wu, J. Zhang, X. Zhang, P. C. Wang, G. Zou and X. J. Liang, *J. Mater. Chem. B*. 2013, **1,** 1109-1118.

56. C. Y. Chen, T. H. Kim, W. C. Wu, C. M. Huang, H. Wei, C. W. Mount, Y. Tian, S. H. Jang, S. H. Pun and A. K. Y. Jen, *Biomaterials.*2013, **34,** 4501-4509.

View Article Online
DOI: 10.1039/C6NJ02753A

57. Y. Li, G. H. Gao and D. S. Lee, *Adv. Healthcare Mater.* 2013, **2,** 388-417.

58. R. P. Johnson, Y. I. Jeong, J. V. John, C. W. Chung, D. H. Kang, M. Selvaraj, H. Suh and I. Kim, *Biomacromolecules.* 2013, **14,** 1434-1443.

59. M. S. C. Hutchinson and L. Helen, Browne, *J. Med. Chem.* 2001, **44,** 1446-1455.

60. R. Huang, Q. C. Wang, X. Y. Zhang, J. Zhu and B. W. Sun, *Biomedicine& Pharmacotherapy.* 2015, **72,** 17-23.

61. K. Virender, M. Goutam, S. Paige, R. Satyanarayna, K. B. Surinder and I. M. Ram, *Mol. Pharmaceutics.* 2015, **12,** 1289-1298.

62. S. Jin, J. X. Wan, L. Z. Meng, X. X. Huang, J. Guo, L. Liu and C. C. Wang, *ACS Appl. Mater. Interfaces.* 2015, **7,** 19843-19852.

63. S. Arpan, S. Sudipa, R. K. Roy, A. W. Satsangi, R. K. Tolcher, B. G. Vadlamudi and L. O. Joo, *Biomaterials.* 2015, **59,** 88-101.

64. X. Wu, Z. Y. Wang, D. Zhu, S. F. Zong, L. P. Yang, Y. Zhong and Y. P. Cui, *ACS Appl. Mater. Interfaces.* 2013, **5,** 10895-10903.

65. B. Y. Qu, X. C. Li, M. Guan, X. Li, L. Hai and Y. Wu, *European Journal of Medicinal Chemistry.* 2014, **72,** 110-118.

66. H. Q. Li, L. J. Shi, J. Wei, C. P. Zhang, Z. T. Zhou and L. Wu, Colloids and Surfaces B: *Biointerfaces*. 2016, **147,** 65-72.

67. T. T. Zuo, Y. Y. Guan, M. L. Chang, F. Zhang, S. S. Lu, T. Wei, W. Shao and G. M. Lin, Colloids and Surfaces B: *Biointerfaces.* 2016, **147,** 90-99.

68. Y. Jiang, L. Y. Lv, H. H. Shi, Y. B. Hua, W. Lv, X. Z. Wang, H. L. Xin and Q. W. Xu, Colloids and Surfaces B: *Biointerfaces.* 2016, **147,** 90-99.

View Article Online
DOI: 10.1039/C6NJ02753A

69. Y. L. Li, Q. P. Qin, Y. C. Liu, Z. F. Chen and H. Liang, *J. Inorg. Biochem.* 2014, **137,** 12-21.

View Article Online
DOI: 10.1039/C6NJ02753A

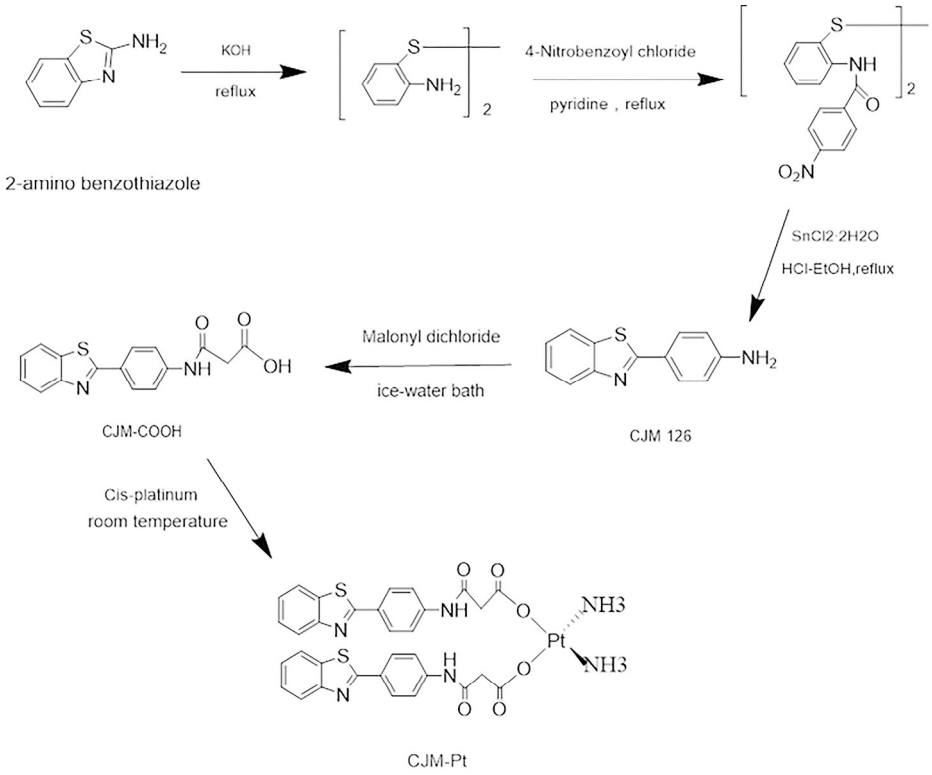

Fig. 1. Overview of synthetic for the synthesis of CJM-Pt.

181x145mm (600 x 600 DPI)

View Article Online
DOI: 10.1039/C6NJ02753A

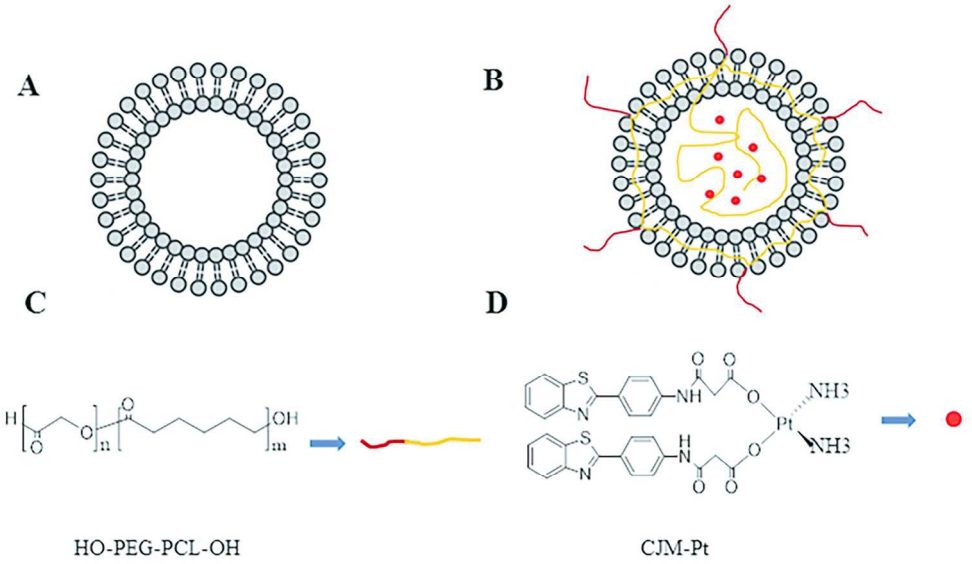

Fig. 2. Pure phosphatide liposomes (A). CJM-Pt loaded liposomes (B). HO-PEG-PCL-OH (C) and CJM-Pt (D).

115x68mm (600 x 600 DPI)

View Article Online
DOI: 10.1039/C6NJ02753A

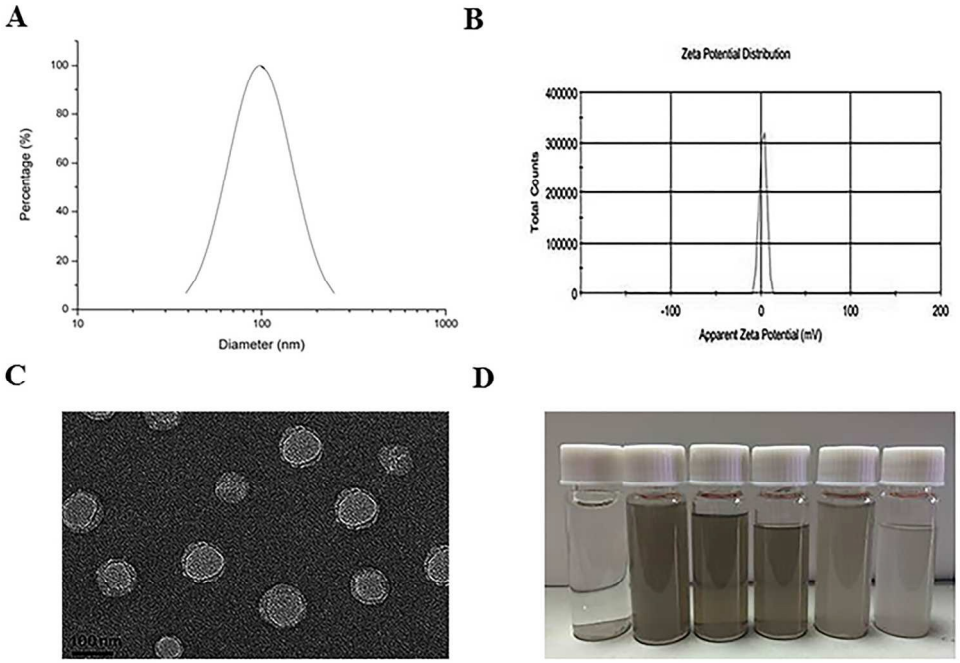

Fig. 3. A, Statistical analysis of the sizes of CJM-Pt loaded liposomes measured from the TEM image. B, The ζ potential of CJM-Pt loaded liposomes. C, TEM image of CJM-Pt loaded liposomes. D, The CJM-Pt loaded liposomes solution under different pH conditions (Pure water, pH=7.4, pH=6.8, pH=6.2, pH=5.7, pH=5.0 from left to right).

142x99mm (600 x 600 DPI)

View Article Online
DOI: 10.1039/C6NJ02753A

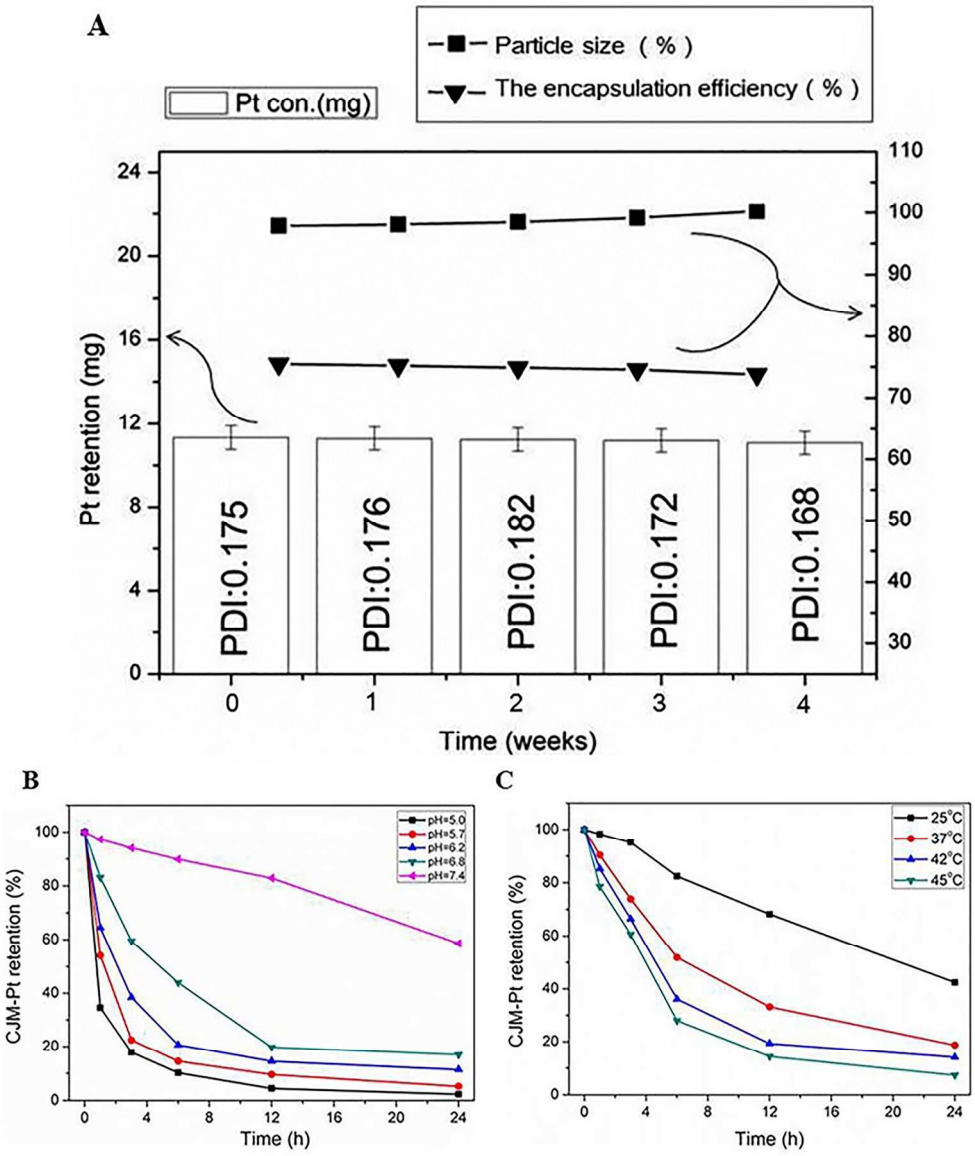

Fig. 4. A, Retention of encapsulated products, change degree of mean particle size and encapsulation efficiency from Lipo-CJM-Pt of weeks. B. pH-responsive release curve of Lipo-CJM-Pt under pH 5.0, 5.7, 6.2, 6.8, 7.4 at 25 ℃. C. Thermo-responsive release curve of Lipo-CJM-Pt at pH 7.4.

236x274mm (300 x 300 DPI)

View Article Online
DOI: 10.1039/C6NJ02753A

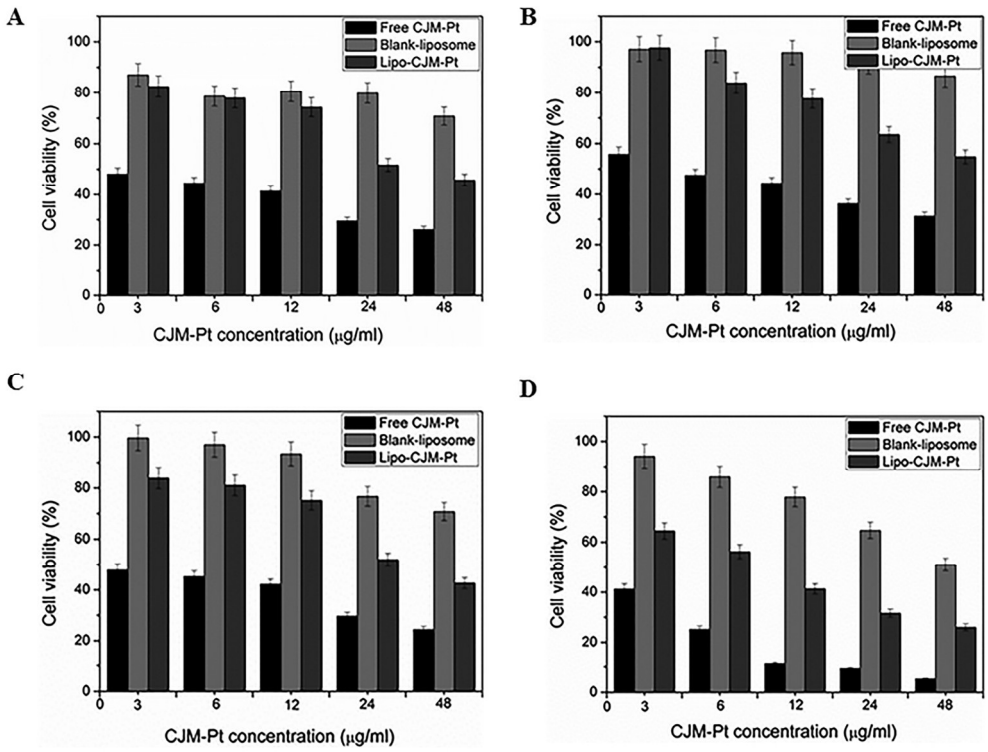

Fig. 5. Relative cell viabilities of MGC-803 (A), SGC-7901 (B), MCF-7 (C) and MDA-MB-231 (D) cells after incubation with CJM-Pt, Blank-liposomes and Lipo-CJM-Pt for 24 h.

167x126mm (300 x 300 DPI)

View Article Online
DOI: 10.1039/C6NJ02753A

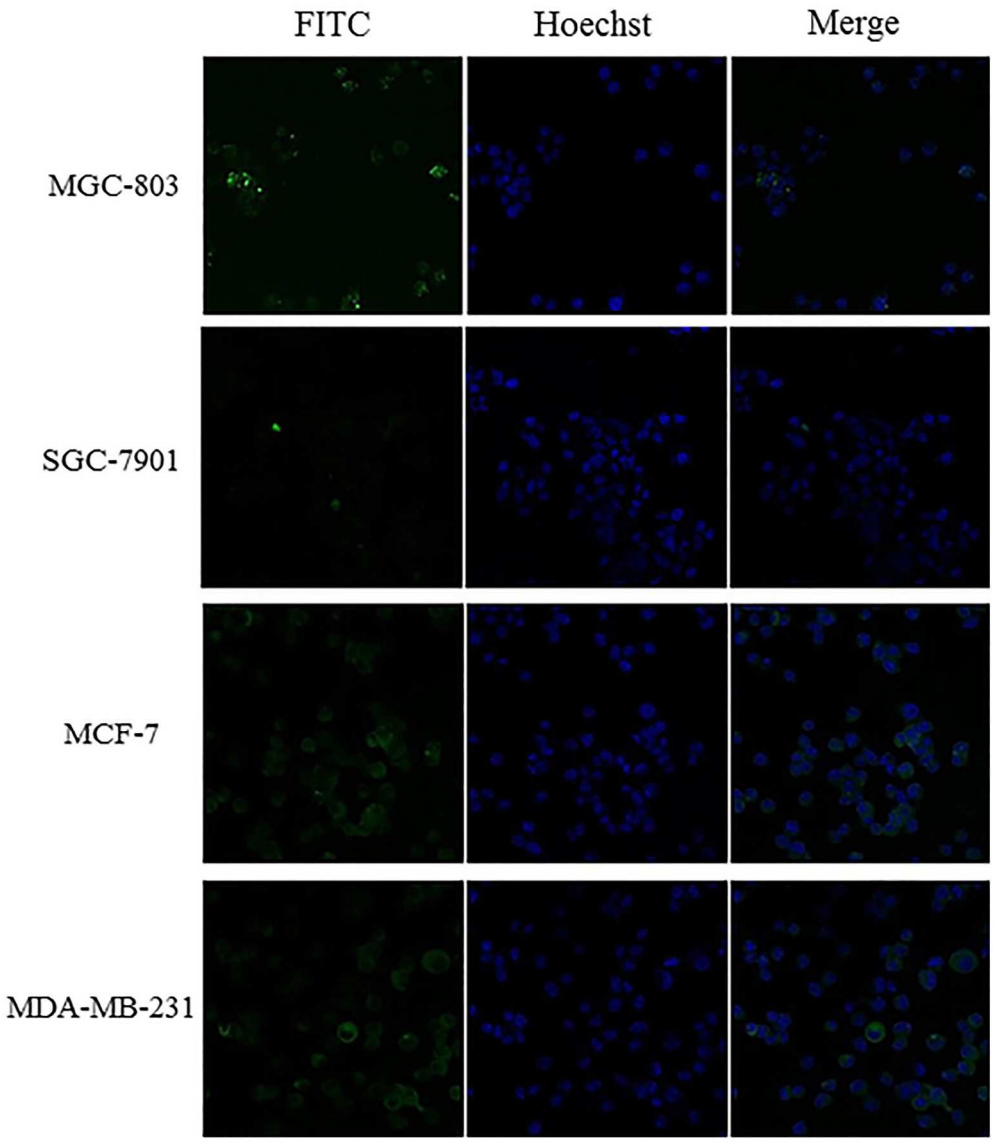

Fig. 6. Binding efficacy of Lipo-CJM-Pt to MGC-803, SGC-7901, MCF-7 and MDA-MB-231 detected by immunofluorescence assay.

176x203mm (600 x 600 DPI)

View Article Online
DOI: 10.1039/C6NJ02753A

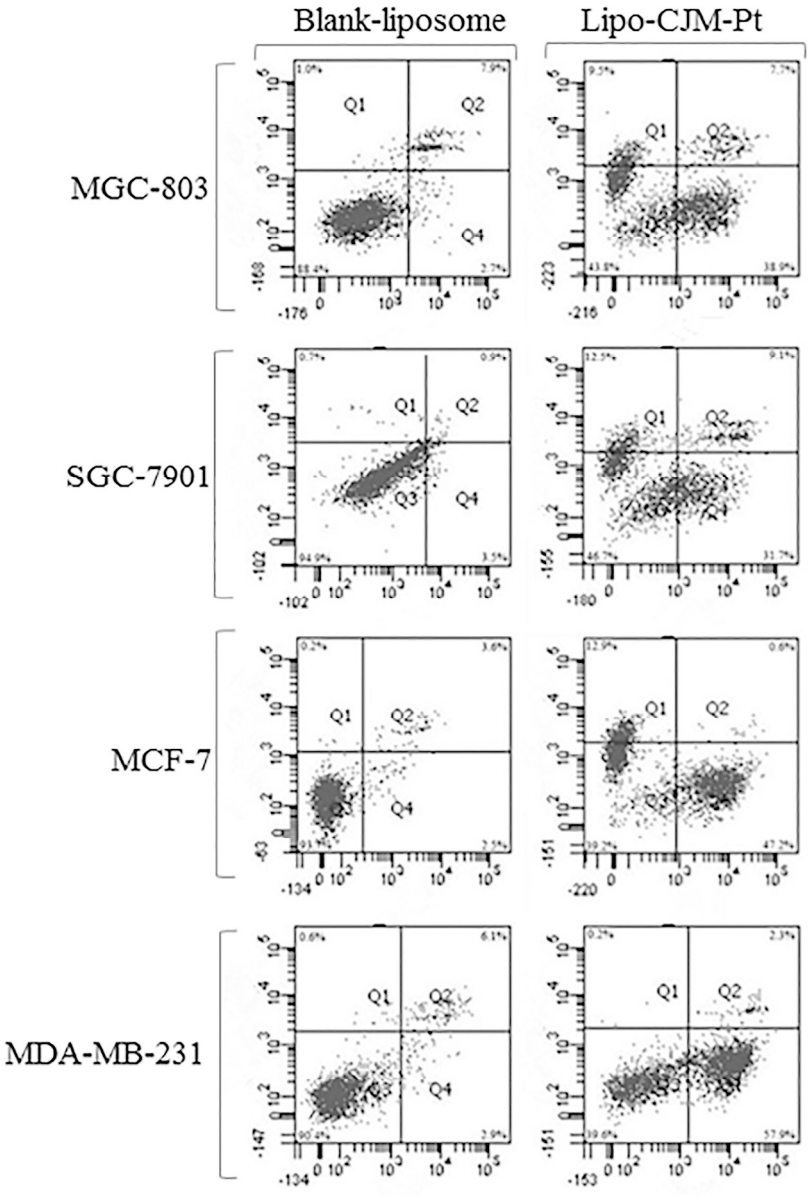

Fig. 7. The apoptosis of MGC-803, SGC-7901, MCF-7 and MDA-MB-231 cells induced by Lipo-CJM-Pt (CJM-Pt equivalent 15 μM) for 24 h.

183x269mm (600 x 600 DPI)

View Article Online
DOI: 10.1039/C6NJ02753A

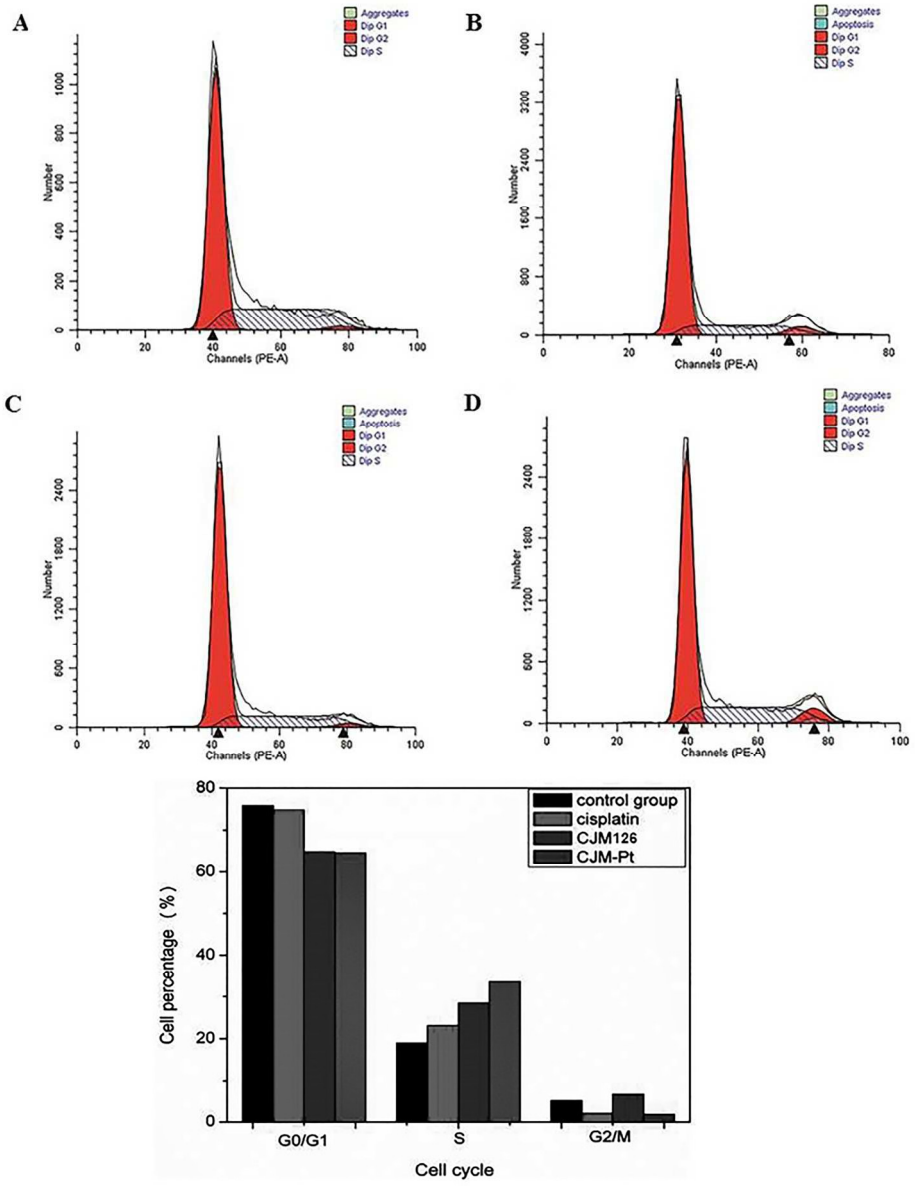

Fig. 8. Effects of cisplatin (B), CJM (C) and CJM-Pt (D) on cell cycle phase arrest in MDA-MB-231 cells. Cells were treated with 15μM of each compound for 24h. Then the cells were fixed and stained with PI to analyze DNA content by flow cytometry.

269x345mm (300 x 300 DPI)

View Article Online
DOI: 10.1039/C6NJ02753A

New Journal of Chemistry

Enhanced cytotoxicity by benzothiazole- containing cisplatin derivative in breast cancer cells

Chaoqun You [a], Jia Yu [a], Yu Sun [a], Yanghui Luo [a], Xiangyang Zhang [b], Jin Zhu [c], Baiwang Sun [a,*]

[a] School of Chemistry and Chemical Engineering, Southeast University, Nanjing 210089, PR China. Fax: +86 25 52090614, Tel: +86 25 52090614, E-mail address: chmsunbw@seu.edu.cn

[b] Laboratory of Organic Chemistry, ETH Zurich, 8093 Zurich, Switzerland

[c] Key Laboratory of Antibody Technique of Ministry of Health, School of Pathology, Nanjing Medical University, Nanjing 210093, PR China

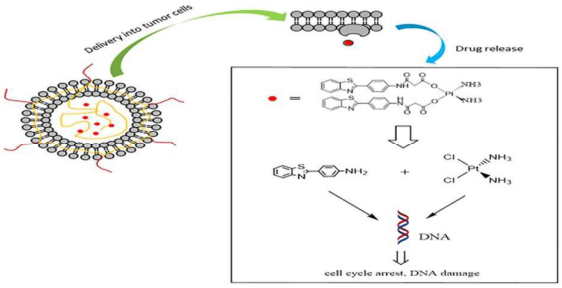

A synergic actional cisplatin derivative via conjugated CJM126 with cisplatin was synthesized and delivery by liposomes to inhibited tumor cells.